Sulphur abundances from the S I near-infrared triplet at 1045 nm [*]

E. Caffau[1], R. Faraggiana[2], P. Bonifacio[3,1,4], H.-G. Ludwig[3,1], and M. Steffen[5]

[1] GEPI, Observatoire de Paris, CNRS, Université Paris Diderot ; Place Jules Janssen 92190 Meudon, France
[2] Università degli Studi di Trieste, Dipartimento di Astronomia, Via Tiepolo 11, I-34131 Trieste, Italy
[3] CIFIST Marie Curie Excellence Team
[4] Istituto Nazionale di Astrofisica - Osservatorio Astronomico di Trieste, Via Tiepolo 11, I-34131 Trieste, Italy
[5] Astrophysikalisches Institut Potsdam, An der Sternwarte 16, D-14482 Potsdam, Germany

ABSTRACT

Context. Unlike silicon and calcium, sulphur is an α-element which does not form dust. Some of the available observations of the evolution of sulphur with metallicity indicate an increased scatter of sulphur to iron ratios at low metallicities or even a bimodal distribution, with some stars showing constant S/Fe at all metallicities and others showing an increasing S/Fe ratio with decreasing metallicity. In metal-poor stars S I lines of Multiplet 1 at 920 nm are not yet too weak to permit to measure the sulphur abundance A(S), however in ground-based observations they are severely affected by telluric lines.

Aims. We investigate the possibility to measure sulphur abundances from S I Mult. 3 at 1045 nm lines, which lie in the near infra-red. These are slightly weaker than those of Mult. 1, but lie in a range not affected by telluric lines.

Methods. We investigate the lines of Mult. 3 in the Sun (G2V), Procyon (F5V), HD 33256 (F5V), HD 25069 (G9V) and ϵ Eri (HD 22049, K2V). For the Sun and Procyon the analysis has been performed with CO^{5}BOLD 3D hydrodynamical model atmospheres, for the other three stars, for which hydrodynamical simulations are not available, the analysis has been performed using 1D model atmospheres.

Results. For our sample of stars we find a global agreement of A(S) from lines of different multiplets.

Conclusions. Our results suggest that the infrared lines of Mult. 3 are a viable indicator of the sulphur abundance which, because of the intrinsic strength of this multiplet, should be suitable to study the trend of [S/Fe] at low metallicities.

Key words. Sun: abundances – Stars: abundances – Galaxy: abundances – Hydrodynamics

1. Introduction

The so-called α-elements (O, Ne, Mg, Si, S, Ca) are among the main products of Type II Supernovae (Woosley & Weaver 1995; Limongi & Chieffi 2003a; Chieffi & Limongi 2004). The iron peak elements are produced by Type II SNe, and it is commonly accepted that Type Ia Supernovae produce similar, or larger amounts of iron-peak elements, and produce little or no α-elements, (Nomoto et al. 1984; Iwamoto et al. 1999). The different timescales for the first explosions of Type II or Type Ia SNe to occur, makes the abundance ratio of α-elements to iron-peak elements a powerful diagnostics of the chemical evolution and star formation history of a galaxy. In the Milky Way, stars of lower metallicity are characterised by higher α-to-iron abundance ratios than found in the Sun and solar metallicity stars

(see, for example, Barbuy 1988; Gratton et al. 2003; Cayrel et al. 2004). This is usually interpreted in terms of a lower contribution of Type Ia SNe. Systems which are characterised by low or bursting star formation, like dwarf galaxies, give time to Type Ia SNe to explode before the enrichment due to Type II SNe has greatly increased. Consequently, such systems display rather low α-to-iron ratios even at low metallicities (see Venn et al. 2004, and references therein) and at solar metallicities, display sub-solar ratios (Bonifacio et al. 2004; Monaco et al. 2005).

One should be aware that the above outlined, simple interpretation of the α-to-iron peak element ratios in terms of products of Type II and Type Ia SNe, relies on the nucleosynthesis computed with 1D explosion models. For Type Ia SNe such computations predict that the original C-O white dwarf is totally burned, mainly to ^{56}Ni. It is interesting to note that in the 2D models by Brown et al. (2005), most of the white dwarf is not burnt and roughly equal masses of ^{56}Ni and ^{28}Si are pro-

duced. It is clear that a different explanation of the α-element enhancement must be sought if these computations are confirmed.

While the theoretical interpretation of the α-to-iron peak ratios is likely still open to debate, it is clear that, from the observational point of view, the abundance of α-elements is an important property of any stellar population. For the study of chemical evolution in external galaxies, the more readily available objects are Blue Compact Galaxies (BCGs) through analysis of their emission line spectra, and Damped Ly-α systems (DLAs) through the analysis of resonance absorption lines. In this way, it is relatively easy to measure sulphur in the gaseous component of both groups of galaxies (Garnett 1989; Centurión et al. 2000).

At variance with Si and Ca, S is a volatile element, and therefore it is not locked into dust grains in the interstellar medium, so that no correction is needed to the measured sulphur abundance. This makes sulphur a more convenient element to trace the α's than either Si or Ca; all three elements are made by oxygen burning, either in a central burning phase, convective shell, or explosive phase. According to Limongi & Chieffi (2003b), there is thus a strong reason to believe that Si, S, and Ca vary in lockstep during the chemical evolution. In spite of this, it is certainly unsatisfactory to compare S/Fe in external galaxies to Si/Fe or Ca/Fe in the Milky Way. It is much more convenient to use a reliable Galactic reference for sulphur abundances, which may be directly compared to measures in external galaxies.

The only way to measure abundances at different metallicities in the Galaxy is to use stars. Unfortunately there are very few sulphur lines which are not blended and remain strong enough to be measured at low metallicities. The lines of Mult. 8[1] (675 nm) and 6 (869 nm) are weak, so only detectable in solar or moderately metal-poor stars, hardly lower than [Fe/H] $\sim$ −1.5 (for the Mult. 8), or −2.0 (for Mult. 6). The lines of Mult. 1 (920 nm) have been recently used to measure A(S)[2] because these lines are strong, and are detectable even at low metallicity. The non-negligible NLTE effects in these lines make them even stronger (Takeda et al. 2005a), therefore more easily measurable. The main problem is that the range in wavelength in which Mult. 1 lies is contaminated by numerous telluric lines. This makes it difficult to obtain all (or at least one) components of Mult. 1 unaffected by telluric absorption.

The 1045 nm lines of Mult. 3 are particularly suited to measure the sulphur abundance. Even if the lines are not as strong as the components of Mult. 1, the big advantage is that there are no telluric lines present in the vicinity of their wavelength. Observing sulphur lines of Mult. 3 provides a possibility to obtain a reliable sulphur abundance in very metal-poor stars.

Existing studies of sulphur in Galactic stars have suggested that in the range −2.5 <[Fe/H]< −2.0 the [S/Fe] ratio shows

either a large scatter or a bimodal behaviour; Most of the stars converge to a "plateau" at about [S/Fe]=+0.4, while a non-negligible number of stars shows a "high" value of [S/Fe] around +0.8. In the sample of Caffau et al. (2005), the determination of [S/Fe] in this range of metallicity is based on the non contaminated lines of Mult. 1. This behaviour has no proposed theoretical interpretation and it may well be due to systematic errors related to the use of Mult. 1. It is therefore of great interest to verify this puzzling finding by the use of an independent and, hopefully better, diagnostics of the sulphur abundance, as can be afforded by the lines of Mult. 3. We moreover recall that these are the only strong S I lines belonging to a triplet system instead of quintet systems as the other S I lines in the visual and near-IR range.

The aim of the paper is to study the S I lines of Mult. 3 in two well known stars – the Sun and Procyon – and to investigate three other bright field stars of spectral type F, G and K: HD 22049, HD 33256, HD 25069 respectively. We compare A(S) from two sulphur lines widely used in sulphur abundance determinations, to the one from Mult. 3 lines. We want to establish Mult. 3 as valuable abundance indicator.

2. Atomic data

The S I lines that we consider in this work, are reported in Table 1. The triplet at 675.7 nm and the line at 869.4 nm have been widely used in the determination of sulphur abundances (see for instance, Nissen et al. 2004; Caffau et al. 2005). The lines of Mult. 3 have not yet been considered[3], except in the Sun (Lambert & Luck 1978; Takeda et al. 2005a). We know that the bluest line of Mult. 3 is blended with an iron line of poorly known $\log gf$, but we nevertheless keep this line for the Sun and Procyon for which we have good observed spectra in hand, and for HD 33256 where A(Fe) is lower than in the Sun, as well as for ϵ Eri where the iron contribution is only 12 % of the total equivalent width (EW); we discard this line for HD 25069 for which the contribution of iron to the total EW is about 18 %, comparable to the error of the EW for this star. In any case, the relative contribution of the iron line to the blend becomes smaller for very metal-poor stars, and thus the line can be a good indicator of the sulphur abundance.

The $\log gf$ value of the Mult. 3 lines, as those of all the other S I lines used here, have been taken from the Kurucz line list; the data are approximately coincident with those from the NIST Atomic Spectra Database (http://physics.nist.gov/PhysRefData/ADS). These gf are experimental values based on three experiments. Owing to the moderate accuracy of the absolute scale, Wiese et al. (1969)

---

[1] We use the Multiplet numbering by Moore (1945)

[2] A(S)=log (N(S)/N(H)) + 12

---

[3] The referee made us aware of a paper (Nissen et al. 2007 astro-ph/0702689, submitted to A&A) which became available through arXiv (arxiv.org) after the submission of this work. The paper describes the first use of the 1045 nm lines for abundance work in metal-poor stars.

Table 1. Atomic parameters of the sulphur lines. Col. (1) is the wavelength; col. (2) the multiplet number; col. (3) the transition; col. (4) the $\log gf$ of the transition taken from the Kurucz line list; col. (5) the excitation energy; col. (6) the Van der Waals damping constant computed at a temperature of 5 500 K according to ABO theory (see Sect. 6) or Kurucz approximation (see text).

Wavelength (nm) air (1)	Mult. (2)	Transition (3)	$\log gf$ (4)	χ_{lo} (eV) (5)	$\log \gamma_6/N_H$ $\left(\text{s}^{-1}\,\text{cm}^3\right)$ (6)
675.6851	8	$^5P_3 - {}^5D^o_2$	–1.76	7.87	–7.146
675.7007	8	$^5P_3 - {}^5D^o_3$	–0.90	7.87	–7.146
675.7171	8	$^5P_3 - {}^5D^o_4$	–0.31	7.87	–7.146
869.3931	6	$^5P_3 - {}^5D^o_3$	–0.51	7.87	–7.337
869.4626	6	$^5P_3 - {}^5D^o_4$	0.08	7.87	–7.337
1045.5449	3	$^3S^o_1 - {}^3P_2$	0.26	6.86	–7.672
1045.6757	3	$^3S^o_1 - {}^3P_0$	–0.43	6.86	–7.672
1045.9406	3	$^3S^o_1 - {}^3P_1$	0.04	6.86	–7.672

renormalised the data theoretically and judged the resulting accuracy of the gf to be within 50 %. In particular we note that all the lines selected for S abundance determination are of D quality, i.e. the uncertainty of the oscillator strength is $\leq 50\,\%$; the lines with highest accuracy (D+, i.e. an uncertainty of the oscillator strength $\leq 40\,\%$) are those of Mult. 1 (920 nm), Mult. 3 (1045 nm), and the line at 869.4 nm of Mult. 6, while the line at 869.3 nm of Mult. 6 is of D quality, as is one component (675.7171 nm) of the 675.7 nm line of Mult. 8. One component of the 675 nm triplet of Mult. 8, the 675.6851 nm line, is of E quality (uncertainty of the oscillator strength > 50 %).

3. Models

For the Sun and Procyon our analysis is based on 3D hydrodynamical model atmospheres computed with the CO⁵BOLD code (Freytag et al. 2002; Wedemeyer et al. 2004). CO⁵BOLD solves the coupled non-linear equations of compressible hydrodynamics in an external gravity field together with non-local frequency-dependent radiation transport for a small volume located at the stellar surface (see CO⁵BOLD manual http://www.astro.uu.se/~bf/cobold/index.html). 25 snapshots were selected from a CO⁵BOLD simulation to represent the photosphere of the Sun (Caffau et al., accepted for A&A Letters), with an effective temperature of 5780 K and covering 6000 s of temporal evolution. 28 snapshots were selected from a 3D simulation of Procyon, having an effective temperature of 6500 K and covering a time interval of 16800 s. Since the timescale of the evolution of the granular flow is about 2.8 times longer in Procyon than in the Sun, the simulated time spans are very similar in a dynamical sense. The Procyon model used in this paper is the same as the one used

by Aufdenberg et al. (2005) in their study of the star's centre-to-limb variation. In both hydrodynamical models, an opacity binning scheme with five wavelength bins was applied for modelling the wavelength-dependence of the radiative transfer (Nordlund 1982; Ludwig et al. 1994; Vögler et al. 2004).

For the other stars we do not have available 3D atmospheres, and therefore used 1D LTE plane-parallel models. Such 1D models were also used as a reference for the Sun and Procyon. In particular:

1. For all the stars we computed hydrostatic 1D model atmospheres computed with the LHD code. LHD is a Lagrangian 1D (assuming plane-parallel geometry) hydrodynamical model atmosphere code. It employs the same micro-physics (equation-of-state, opacities) as CO⁵BOLD. The convective energy transport is described by mixing-length theory. The spatial discretisation and numerical solution of the radiative transfer equation is similar to the one in CO⁵BOLD, albeit simplified for the 1D geometry. The wavelength-dependence of the radiation field is treated by the opacity binning method. A hydrostatic stratification in radiative-convective equilibrium is obtained by following the actual thermal and dynamical evolution in time of the atmosphere until a stationary state is reached. LHD produces standard 1D model atmospheres which are differentially comparable to corresponding 3D CO⁵BOLD models. Remaining choices entering an LHD model calculation are the value of the mixing-length parameter, which formulation of mixing-length theory to use, and in which way turbulent pressure is treated in the momentum equation. Note, that these degrees of freedom are also present in other 1D model atmosphere codes. The LHD models presented in this work have all been computed with $\alpha_{\text{MLT}} = 1.5$ using the formulation of Mihalas (1978), and turbulent pressure has been neglected. Comparisons to 3D models were always made with LHD models having the same effective temperature, gravity, and chemical composition as the 3D model.

2. For all stars, except the Sun, we computed ATLAS9 (Kurucz 1993a, 2005a) models using the Linux version (Sbordone et al. 2004; Sbordone 2005) of the code. All these models have been computed with the "NEW" Opacity Distribution Functions (Castelli & Kurucz 2003), which are based on solar abundances from Grevesse & Sauval (1998) with $1\,\text{km s}^{-1}$ micro-turbulence, a mixing-length parameter α_{MLT} of 1.25 and no overshooting.

3. We used an ATLAS9 (Kurucz 1993a, 2005a) model of the Sun computed by Fiorella Castelli with the solar abundances of Asplund et al. (2005) as input for the chemical composition. The Opacity Distribution Functions were explicitly computed for the same chemical composition and a micro-turbulent velocity of $1\,\text{km s}^{-1}$. The model was computed assuming a mixing-length parameter of 1.25 and no overshooting.

It is available at http://wwwuser.oats.inaf.it/castelli/sun/ap00t5777g44377k1asp.dat.

4. We used the Holweger-Müller solar model (Holweger 1967; Holweger & Mueller 1974). It is an empirical model of the solar photosphere and lower chromosphere assuming LTE, and largely reproducing the Sun's continuous and line spectrum. It considers 900 selected line profiles of 31 atoms and ions.

5. For the Sun and Procyon we considered horizontal and temporal averages of the 3D snapshots over surfaces of equal (Rosseland) optical depth. Comparison with these averaged 3D models, henceforth denoted as ⟨3D⟩ models, provide estimates of the influence of fluctuations around the mean stratification on the line formation process. Comparing 3D and 1D models of this kind is largely independent of arbitrary assumptions entering the constructions of standard 1D models. The only free parameter which has to be specified for the 1D average model is the micro-turbulence to be used in related spectrum synthesis calculations.

The spectral synthesis calculations for the CO^{5}BOLD, LHD, ATLAS and Holweger-Müller models were performed with the code Linfor3D (see http://www.aip.de/~mst/Linfor3D/linfor_3D_manual.pdf); for ATLAS models we also used SYNTHE (Kurucz 1993b, 2005a), in its Linux version (Sbordone et al. 2004; Sbordone 2005). This was used in the cases in which we wanted to compute a synthetic spectrum containing many lines from other atoms and molecules, to fit the observed data. The present version of Linfor3D can handle at maximum a few tens of lines at a time, while SYNTHE does not suffer such a limitation.

4. 3D abundance corrections

The purpose of analysing a star both with 3D hydrodynamical models and 1D models is to derive "3D abundance corrections" which may be used to correct the analysis of other stars of similar atmospheric parameters, performed in 1D. It is clear that from the computational point of view 1D modelling (both model atmosphere and spectrum synthesis) is much more convenient than 3D modelling. It is unlikely that in the near future the computing power will increase to the level that 3D analysis of stellar spectra will be done routinely. On the other hand it is conceivable that grids of hydrodynamical models will be constructed from which "3D corrections" can be computed, and these can be used to correct the results of a 1D analysis. It is therefore important to define what is meant by a "3D correction". In this paper we give 3D-1D abundance corrections with reference to LHD models. These provide a reasonably well-defined way to establish the relation between a 3D hydrodynamical and 1D hydrostatic model. The fact that LHD and CO^{5}BOLD use the same opacities and micro-physics ensures that the differences reflect *only* the 3D effects and no other

effects, as would be the case if we computed corrections with respect to other hydrostatic models, like ATLAS. It may be useful to summarise the differences between a 3D hydrodynamic model and a 1D hydrostatic model as due to two factors:

1. a different mean structure of the two classes of models;
2. horizontal temperature and pressure fluctuations, which are present in a 3D simulation but not (by definition) in a 1D model.

Our definition of "3D correction" is made in order to take into account both effects at the same time.

If one wants to see the difference in abundance due *only* to the different mean temperature structure one may compare the abundances derived from the horizontally and temporally averaged 3D model, which we defined above as the ⟨3D⟩ model, to the corresponding LHD model. On the other hand, if one wants to evaluate *only* the effect of horizontal temperature and fluctuations, it is more appropriate to compare the 3D abundances with those derived from the ⟨3D⟩ model.

5. Data

For the Sun we considered two high resolution, high signal to noise ratio, spectra of the solar flux.

1. The spectrum we will refer to as "Kurucz flux" is based on fifty solar Fourier transform spectrometer (FTS) scans taken by J. Brault and L. Testerman at Kitt Peak, with a spectral resolution of the order of 300 000 and signal to noise of around 3 000, varying from range to range (further details can be found in Kurucz 2005b).

2. The "Neckel flux" refers to the Neckel & Labs (1984) absolutely calibrated FTS spectra obtained at Kitt Peak, covering the range 330 nm to 1250 nm. The spectral purity ranges from 0.4 pm at 330 nm to 2 pm at 1250 nm. This means that the resolution at 1045 nm is about 500 000.

The spectra for Procyon and the other stars were obtained from the UVES Paranal Observatory Project (Bagnulo et al. 2003). For the 670 nm and the 870 nm lines, we have taken the reduced data present in the UVES POP web site[4], the spectral resolution is of about 80 000. The lines of Mult. 3 are not available in the POP reduced spectra, although inspection of the raw data reveals that these wavelengths are indeed recorded on the MIT CCD of UVES in the standard 860 nm setting, but the number of counts is very low (UVES is very inefficient at these wavelengths) and only about 1/3 of the order is present on the CCD. For these two reasons a standard extraction with the UVES pipeline fails to extract this order. We downloaded the raw data and associated calibration observations from the ESO archive and reduced them using the UVES pipeline. We forced the extraction of the last order in the 860 nm setting by declaring the number of orders to be found. This allowed a satisfactory order definition and subsequent order extraction.

[4] http://www.sc.eso.org/santiago/uvespop/

6. Data analysis

To derive sulphur abundances we measured the equivalent width (EW) of the selected sulphur lines and, when possible, fitted the line profiles.

For the triplet lines, EWs were computed by direct numerical integration using the trapeze sum rule, or with the integration of a fitted Gaussian for weak lines or Voigt profile for strong lines, using the IRAF task `splot`.

All line profile fitting has been performed using a code, described in Caffau et al. (2005), which performs a χ^2 minimisation of the deviation between synthetic profiles and the observed spectrum. In the fitting, the sulphur abundance, the level of the continuum, and a wavelength shift are left as free parameters, while the macro-turbulence has to be fixed *a priori*.

When available, for the Van der Waals broadening we used the parameter derived from the theory by Anstee & O'Mara (1995); Barklem & O'Mara (1997); Barklem et al. (1998b) and summarised in Barklem et al. (1998a); in this paper we collectively refer to this work as "ABO" theory. Otherwise we relied on the approximation build into the SYNTHE spectrum synthesis suite (Kurucz 1993b, 2005a). The comparison of this approximation to other ones can be found in Ryan (1998), who refers to its use in the WIDTH code (Kurucz 2005a). We note here that the approximation is used in SYNTHE and WIDTH for all lines for which literature data on the Van der Walls broadening do not exist, and not only for iron-peak elements, as the reader might be induced to believe reading the paper of Ryan (1998).

We used a 3D CO^{5}BOLD simulation for the sulphur analysis in the Sun and Procyon. For ϵ Eri (HD 22049) we computed the 3D-1D abundance corrections by using a CO^{5}BOLD simulation whose parameters (T_{eff}=5073 K, log g=4.42, [M/H]=0.0) were very close to its stellar parameters.

6.1. Corrections for departure from local thermodynamic equilibrium

According to Takeda et al. (2005a) several of the atomic sulphur lines show non-negligible departures from LTE. It is beyond the purpose of this paper to investigate these departures, however we shall make use of the published departures from LTE of Takeda et al. (2005a).

7. Results for the individual stars

7.1. Sun

For the Sun we consider the 675.7 nm triplet of Mult. 8, the 869 nm lines of Mult. 6 and the three lines of Mult. 3 even if we know that the bluest is blended.

The results are reported in Table 2 and are: the EW for each feature (second column), the sulphur abundance derived from the EWs and the results for the 3D corrections, assuming a micro-turbulence ξ_{micro} of 1.5 km s^{-1} and 1.0 km s^{-1} in the 1D models. The 3D corrections are always defined with respect to the corresponding 1D LHD model. In LTE, the 3D abundance corrections for the Sun turn out to be small. By magnitude this is compatible with the findings of Nissen et al. (2004), however, our corrections have opposite sign. It is quite likely that the difference comes about by the different choice of 1D reference atmosphere to which the corrections are related. In fact, Nissen et al. (2004) used a MARCS model as the 1D reference. In the table the NLTE correction, according to Takeda et al. (2005a), is included in the last but one column (Δ). The last column is the adopted sulphur abundance. In columns 4-11 there are the sulphur abundance values derived from 1D models, using a ξ_{micro} of 1.0 and 1.5 km s^{-1}.

In Fig. 1 the solar sulphur lines considered in this work are plotted together with the 3D synthetic spectra. The weak lines of Mult. 6 and Mult. 8 have also been fitted with both the CO^{5}BOLD+Linfor3D synthetic spectra and ATLAS9+SYNTHE. The results are, within 0.05 dex, in agreement with the abundances obtained from the EWs.

The LTE computation implies A(S)=7.252 ± 0.143 (this is an average of all the A(S) given in column (3) of Table 2), while applying the NLTE corrections of Takeda et al. (2005a) (given in column (11) of Table 2) we obtain A(S)=7.213 ± 0.113; the quoted errors are the line to line scatter in the abundance determinations from the six features considered. It is worth pointing out that, given the high S/N of the available solar spectra, the associated statistical errors are negligible. Therefore the line to line scatter must reflect inadequacies in the model atmospheres and/or the line formation calculations, and/or errors in the atomic data.

Examining more closely the disagreement between lines, we note that the 869.3 nm line is blended with molecular lines (C$_2$ and CN) whose contribution we estimated to be of the order of 15 %, and which was consequently subtracted from the EW. However, considering the uncertainties in the log gf of these molecular lines, it is probably safer to discard this line. From the 675.7 nm triplet we find A(S)=7.136 ± 0.004 (where the error is now the standard deviation between the measures from the two observed solar spectra), while the sulphur abundance is 7.204 ± 0.021 in LTE and 7.194 ± 0.021 in NLTE for the 869.4 nm line. From Mult. 3 we find A(S)=7.379 ± 0.014 in LTE and A(S)=7.309 ± 0.016 in NLTE. There is an obvious trend in A(S) with EW. Note that since this result is obtained using 3D atmospheres we cannot invoke a micro-turbulent velocity to remove this trend. This effect could be explained if 3D-NLTE corrections are larger than the published 1D-NLTE corrections, adopted here. If this were the case, the solar S abundance should be A(S)=7.14, as indicated by the 675.7 nm triplet, which is virtually unaffected by NLTE. This result is also supported by the analysis of [SI] line at 1082 nm (Caffau & Ludwig, in press), whose departure from LTE is negligible, from which the sulphur abundance is 7.14. However, the trend could have other explanations. At least in part, the line broad-

Table 2. Solar sulphur abundances from flux spectra. Col. (1) is the wavelength of the line followed by an identification flag, K means Kurucz flux, N Neckel flux; col. (2) is the Equivalent Width; col. (3) is the sulphur abundance, A(S), according to the CO^{5}BOLD 3D model; col. (4) to (11) give the abundances for a micro-turbulence of 1.5 and 1.0 km s^{-1} for the ⟨3D⟩, ATLAS, HM, and LHD model, respectively; col. (12) and (13) provide the 3D abundance corrections relative to the LHD model for a micro-turbulence of 1.5 and 1.0 km s^{-1}, respectively; col. (14) is the NLTE correction from Takeda et al. (2005a); col. (15) the A(S) we finally adopted. LHD models were computed with α_{MLT} of 1.5, ATLAS models with α_{MLT} of 1.25.

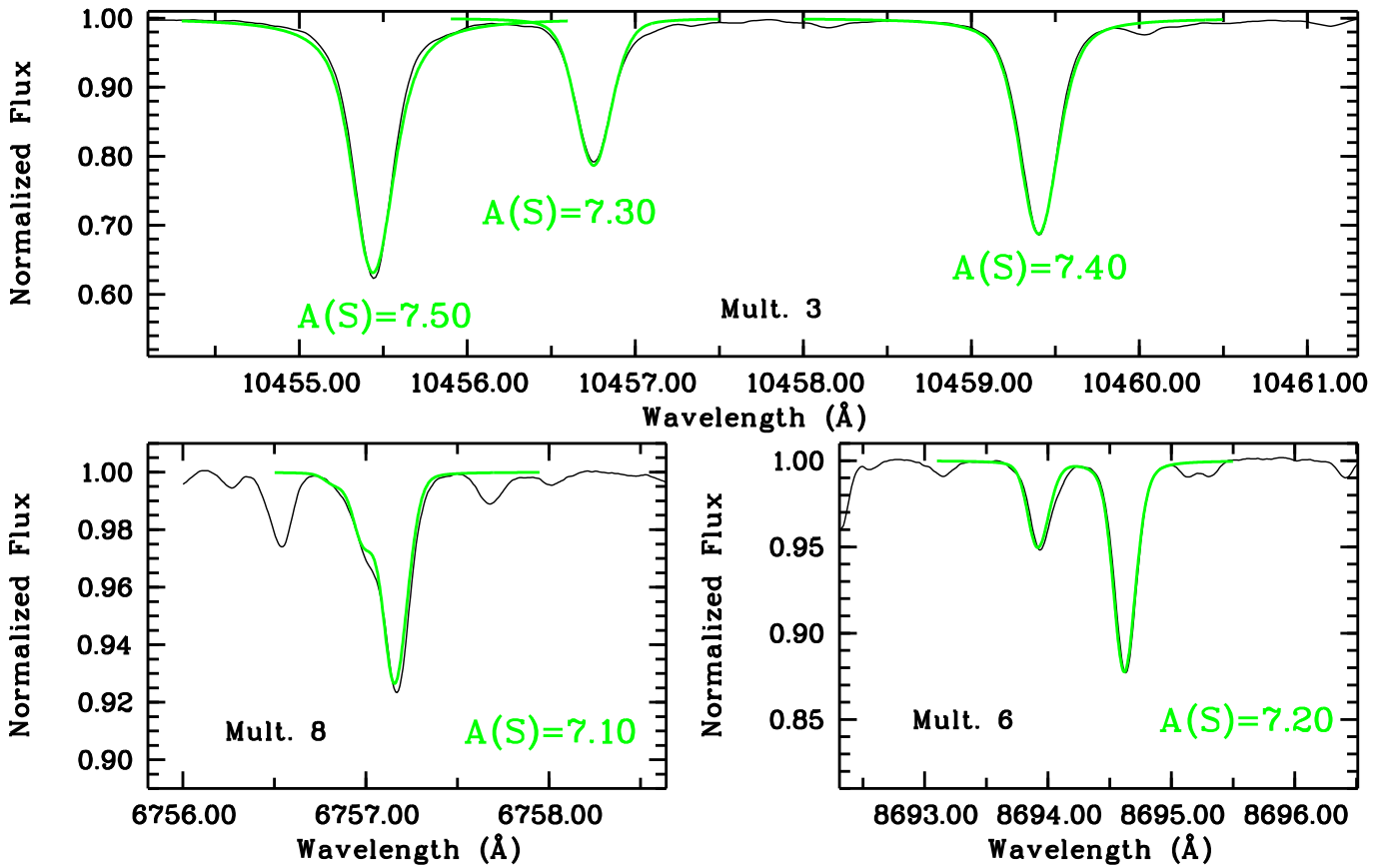| Wave nm	EW pm	3D	⟨3D⟩		ATLAS		HM		LHD		3D-LHD		Δ	A(S)
			1.5	1.0	1.5	1.0	1.5	1.0	1.5	1.0	1.5	1.0		
(1)	(2)	(3)	(4)	(5)	(6)	(7)	(8)	(9)	(10)	(11)	(12)	(13)	(14)	(15)
675.7K	1.805	7.138	7.142	7.151	7.130	7.137	7.168	7.176	7.121	7.129	0.017	0.009		7.138
675.7N	1.789	7.133	7.137	7.146	7.125	7.132	7.163	7.171	7.116	7.124	0.017	0.009		7.133
869.3K	0.844	7.028	7.036	7.042	7.028	7.033	7.059	7.064	7.018	7.023	0.010	0.005	-0.010	7.018
869.3N	0.863	7.040	7.048	7.054	7.040	7.045	7.070	7.076	7.030	7.035	0.010	0.005	-0.010	7.030
869.4K	3.025	7.189	7.177	7.196	7.153	7.169	7.182	7.202	7.144	7.161	0.045	0.028	-0.010	7.179
869.4N	3.157	7.219	7.206	7.225	7.182	7.198	7.215	7.236	7.173	7.190	0.046	0.029	-0.010	7.209
1045.5K	13.660	7.402	7.320	7.378	7.277	7.330	7.346	7.405	7.266	7.321	0.136	0.081	-0.090	7.312
1045.5N	13.450	7.383	7.302	7.360	7.259	7.312	7.328	7.386	7.247	7.303	0.136	0.080	-0.090	7.293
1045.6K	6.872	7.387	7.326	7.374	7.298	7.342	7.333	7.382	7.288	7.332	0.099	0.055	-0.050	7.337
1045.6N	6.725	7.366	7.306	7.353	7.279	7.322	7.313	7.362	7.269	7.312	0.098	0.054	-0.050	7.316
1045.9K	10.650	7.370	7.292	7.347	7.254	7.306	7.307	7.364	7.244	7.298	0.126	0.073	-0.070	7.300
1045.9N	10.610	7.366	7.288	7.343	7.250	7.302	7.303	7.360	7.240	7.293	0.126	0.073	-0.070	7.296

Fig. 1. Sun: synthetic spectra (green/grey thick solid line) based on the 3D model atmosphere are over-imposed on the observed (black solid line) solar flux spectrum of Kurucz.
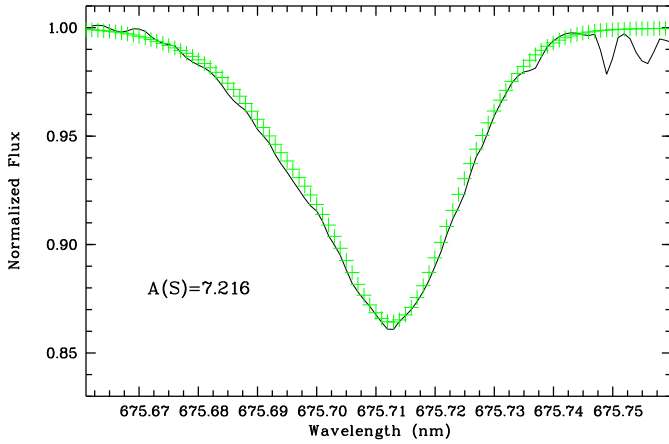
Fig. 2. Procyon: the 3D fit (green/grey crosses) is over-imposed on the observed spectrum (black solid line) for the S I 675.7 nm triplet.

ening theory employed could be inadequate, as could be the case for the hydrodynamic velocity and temperature field of the CO⁵BOLD simulation. Finally, we note that Asplund et al. (2005) find a solar LTE sulphur abundance of A(S)=7.14±0.05.

7.2. Procyon

For Procyon we adopt the stellar parameters derived by Steffen (1985), that is $T_{\rm eff}$ = 6500 K, log g=4.0 and solar metallicity. These stellar parameters are very close to the results of the most recent determination due to Aufdenberg et al. (2005), who find $T_{\rm eff}$=6516 ± 87 K, log g=3.95 ± 0.02. For Mult. 8 and Mult. 6 we measure S/N=400, for Mult. 3 S/N=50.

For the 3D fitting we assumed a Gaussian instrumental broadening with FWHM of 3.75 km s^{-1}, corresponding to a spectral resolution of 80 000.

The results are reported in Table 3. In the second column the EW is given, the next five columns show the sulphur abundance computed from EWs. The next two columns show the sulphur abundance from line profile fitting (see in Fig. 2 the fit of the 675.7 nm triplet); the two lines (869.3931 nm and 869.4626 nm line) of Mult. 6 are fitted at the same time. In column (10) the 3D-1D correction is given, in column (11), when available, the NLTE correction according to Takeda et al. (2005a) is reported. In the last but one column the adopted sulphur abundance is given.

The standard deviation of the EW related to the finite S/N is computed according to Cayrel's formula (Cayrel 1988):

$$\epsilon \, (\text{EW}) = 1.6 \times \frac{\sqrt{\text{FWHM} \times \text{PixelSize}}}{S/N} \qquad (1)$$

where S/N is the signal to noise value, FWHM is the full width at half maximum of the line, PixelSize is the size of the detector pixel in wavelength units. From the errors of the EWs we computed the corresponding errors of A(S) using the curve of growth of each line. These errors are provided in the last column of Table 3.

For Procyon the 3D corrections are definitely not negligible, above all for the strong lines of Mult. 3. This effect is not so evident in the Sun which is cooler than Procyon. We shall see that the 3D corrections are negligible in the cooler ϵ Eri (see Table 6). We note that the 3D corrections given in Tab. 3 are positive, implying that – for a given abundance – the same lines are weaker in 3D than in 1D. This behaviour is opposite to the findings by Steffen & Holweger (2002) who argue that in general one should expect a strengthening of lines in 3D atmospheres. However, their argumentation is not strict, and actually refers to the 3D-⟨3D⟩ correction for weak (unsaturated) lines in the Sun. In fact, the weaker lines in Tab. 2 comply with the expected line strengthening in 3D.

The fact that the difference of the 3D abundance to that derived from the ⟨3D⟩ model (col. (3) – col. (4) in Tab. 3) is of similar size as the total 3D-1D correction given in col. (9) (col. (3) – col. (6) in Tab. 3) shows that the pronounced line weakening cannot be the result of a different mean temperature structure in 3D with respect to 1D. In fact the abundances derived from the ⟨3D⟩ (col. (4)) and the LHD model (col. (6)) are very similar. Rather the line weakening must be caused by the sizable horizontal temperature fluctuations present in the photosphere of Procyon, or by a substantially different effective micro-turbulence in 3D and 1D, respectively.

In order to explore this question somewhat further, Figures 3 and 4 depict the joint probability density of the (disk-centre) EW of the 1045.9 nm line and the neighbouring continuum intensity for the Procyon and solar 3D model, respectively. The contours illustrate the correlation between continuum intensity and EW over the stellar surface. We find a bimodal distribution in the solar case, a single peak and diffuse "halo" in the case of Procyon. The difference can be traced back to qualitatively different formation heights of the line. In the case of the Sun the largest contribution to the line absorption stems from the granular layers as such, while the maximum contribution is shifted to higher layers of reverse granulation in Procyon. While in the Sun temperature fluctuations in the continuum formation layers are positively correlated with the temperature fluctuations in the line forming layers, we typically find an anti-correlation in Procyon. Due to the high excitation potential of the lower level the line is rather temperature sensitive. In the Sun instances of high continuum intensity coincide with a high temperature in the line forming layers. Higher temperatures increase the population of the lower level of the transition leading to a stronger line. The reverse happens in moments of low continuum intensity. In Procyon, the line still tends to become stronger with increasing continuum intensity. However, the anti-correlation between continuum intensity and temperature in parts of the line forming layers leads to a smaller variation of the line strength.

The ⟨3D⟩ average and the LHD model indicated by symbols in Fig. 3 point towards a potential problem in our de-

Table 3. Sulphur abundances in Procyon. Col. (1) is the wavelength of the line; col. (2) is the Equivalent Width; col. (3) is the sulphur abundance, A(S), according to the CO^{5}BOLD 3D model; col. (4) is A(S) from the ⟨3D⟩ model; col. (5) is A(S) from the ATLAS 1D model; col. (6) is A(S) from the LHD 1D model; col. (7) and (8) are the A(S) from fitting using a CO^{5}BOLD 3D and a ATLAS+SYNTHE grid, respectively; in all 1D models a micro-turbulence of 2.1 km s^{-1} was assumed; col. (9) is the 3D correction; col. (10) is the NLTE correction from Takeda et al. (2005a); col. (11) is the A(S) we adopted; col. (12) is the statistical error. α_{MLT} is of 1.50 for the LHD model and 1.25 for the ATLAS model.

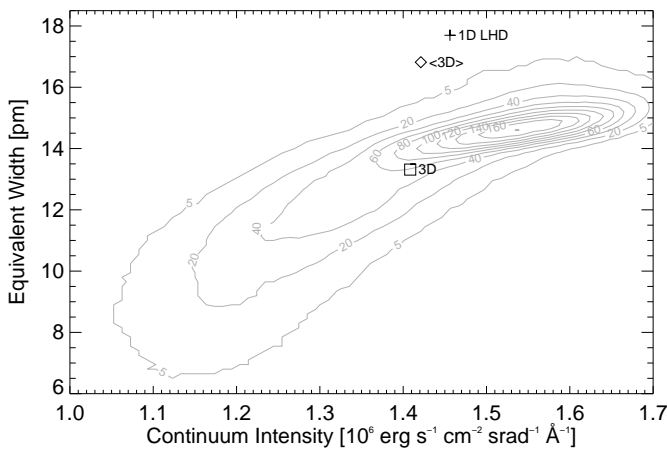| Wavelength (nm) (1)	EW (pm) (2)	A(S) from EW				A(S) from fit		3D-LHD (9)	Δ (10)	A(S) (11)	σ (12)
		3D (3)	⟨3D⟩ (4)	ATLAS (5)	LHD (6)	3D (7)	ATSY (8)				
675.7	4.371	7.231	7.197	7.141	7.177	7.216	7.162	0.053		7.231	0.005
869.3	3.182	7.332	7.298	7.239	7.273	7.257	7.214	0.059	-0.038	7.294	0.005
869.4	6.007	7.265	7.187	7.120	7.138			0.128	-0.057	7.268	0.005
1045.5	18.000	7.557	7.352	7.326	7.274			0.284	-0.271	7.286	0.030
1045.6	10.180	7.410	7.242	7.193	7.178			0.233	-0.135	7.275	0.040
1045.9	15.370	7.547	7.334	7.302	7.258	7.199		0.289	-0.231	7.316	0.030

Fig. 3. Procyon: joint probability density function (not normalised) of continuum intensity and (disk-centre) EW for the 1045.9 nm line in the 3D model (grey contours). The labelled symbols mark the 3D and ⟨3D⟩ average, as well as the result for a LHD model with α_{MLT}=1.5. The micro-turbulent velocity for the 1D models is 2.1 km s^{-1}.

Fig. 4. Sun: same as Fig. 3 for the solar case. The micro-turbulent velocity for the 1D models is 1.0 km s^{-1}.

termination of 3D abundance corrections for Procyon. None of the about 6×10^4 vertical profiles entering the calculation of the probability density corresponds to the ⟨3D⟩ model – at least as far as it concerns the line formation properties. The same holds for the LHD model. It appears plausible that the micro-turbulence prescribed in 1D line formation calculations – motivated from observations – is too large in comparison to the effective micro-turbulence intrinsic to the 3D model. We note here that our adopted micro-turbulence of 2.1 km s^{-1} from Steffen (1985) is in agreement, within quoted errors, with those of Fuhrmann (1998); Gratton et al. (1996); Takeda et al. (1998) and Allende Prieto et al. (2002), while Takeda et al. (1996) pre-
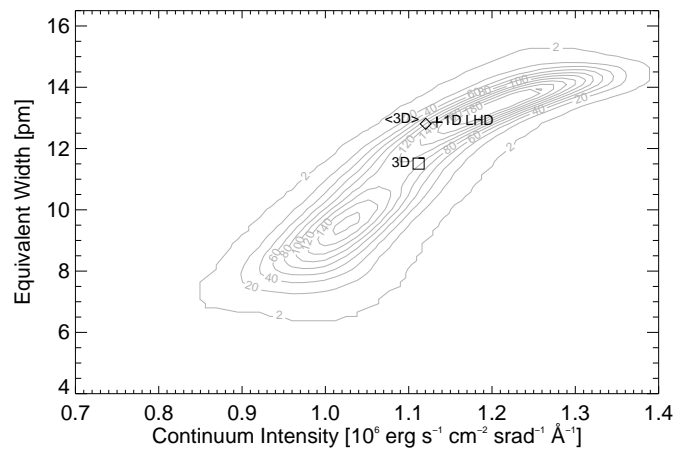
fer a lower value of 1.4 km s^{-1}. Test calculations have shown that a reduction on ξ_{micro} from 2.1 km s^{-1} to 1.5 km s^{-1} leads to a reduction of the abundance correction 3D-LHD by a factor of two. In part, this may explain the different 3D corrections we obtain in comparison to Nissen et al. (2004) who find negligible corrections for an only slightly cooler atmosphere (T_{eff}=6191 K, log g=4.04, [M/H]=0.0). On the other hand, all sulphur lines which span a range of a factor five in equivalent width provide a consistent abundance in 3D when 1D-NLTE effects are included. We cannot provide a resolution here, but the issue of the appropriate micro-turbulence in 3D-1D comparisons clearly needs further investigation.

In LTE we obtain a sulphur abundance of 7.400 ± 0.131, while including NLTE corrections it becomes 7.278 ± 0.029. Once NLTE corrections are applied the scatter becomes tiny and fully compatible with the noise in the data. We commented

before that the 869.3 nm line is blended by molecular lines. If we discard this line A(S)=7.250 ± 0.026. Thus, the difference is small. This is perhaps not surprising, since Procyon is hotter than the Sun, and molecular lines are less prominent in this spectral range.

7.3. HD 33256

The stellar parameters found in the literature for this star show little scatter. We assume $T_{\rm eff}$ = 6 454 K, which we derived by fitting the Hα wings with a grid of synthetic spectra computed with ATLAS+SYNTHE. We recall that the SYNTHE code computes the van der Waals broadening of the Balmer lines according to the theory of Ali & Griem (1965), and the Stark broadening according to Vidal et al. (1973). Had we adopted the broadening theory of Barklem et al. (2000) we would have obtained a lower effective temperature, as pointed out e.g. by Bonifacio et al. (2007). We assumed the stellar parameters log g = 4.00, $V \sin(i)$= 10 km s^{-1}, $\xi_{\rm micro}$ = 1.55 km s^{-1}. From 20 Fe I lines we obtain [Fe/H] = 7.25 ± 0.11; 18 lines of Fe II give [Fe/H] = 7.29 ± 0.15. For the ranges at 600 nm and 800 nm we measure a S/N ratio of about 700, and S/N = 25 around 1045 nm.

The results of our analysis are listed in Table 4. The errors of A(S), derived from these S/N ratios according to the formula (1), are given in the last column of the table.

The LTE sulphur abundance is 7.022 ± 0.183; applying the Takeda et al. (2005a) NLTE corrections A(S)=6.900 ± 0.091. After applying the NLTE corrections the line to line scatter is fully compatible with the expected measurement errors. The sulphur abundance with NLTE correction from the lines of Mult. 3 is 6.938 ± 0.123, to be compared with A(S)=6.862 ± 0.033 if we consider the 675.7 nm, 869.3 nm and 869.4 nm lines, or A(S)=6.861 ± 0.047 if we consider only the two lines of Mult. 6. As can be seen, the sulphur abundances obtained from the different lines are in agreement within one standard deviation.

7.4. HD 25069

We adopted the stellar parameter from Valenti & Fischer (2005) ($T_{\rm eff}$ = 4 994 K, log g = 3.53, and [Fe/H]=+0.10).

The fit of the 675.7 nm triplet gives A(S)=7.249, but, due to the presence of a distortion in the line profile, the fit was performed in a range not including the blue wing of the line.

S/N is 500 for the 600 nm and 800 nm ranges. In the range 1045 nm we measure S/N=28. EWs and sulphur abundances are reported in Table 5. The errors according formula (1) are provided in the last column of Table 5.

For this star the IR line at 1045.9 nm appears to have an unusual shape, the core appears broad and flat, unlike the other atomic lines in this spectrum, for this reason we rejected this line. The triplet at 675.7 nm should also be rejected because the line profile appears distorted, possibly by a cosmic ray hit.

For this star the contribution of the iron line to the 1045.5 nm line of Mult. 3 is large. So considering only the 869.4 nm and the 1045.6 nm line, the sulphur abundance is 7.297 ± 0.106, and 7.248 ± 0.070 if we apply the NLTE corrections of Takeda et al. (2005a). Considering all lines A(S)=7.254 ± 0.102 in LTE, A(S)=7.207 ± 0.120 with NLTE corrections of Takeda et al. (2005a).

Since A(S)=7.199 from the 869.4 nm line, and A(S)=7.169 ± 0.182 from the the two lines considered in Mult.3, we can conclude that the abundance determinations from the two lines are in good agreement. We attribute the abundance difference of 0.26 dex between the lines at 1045.6 and 1045.9 nm to the low S/N of the spectrum of Mult. 3.

7.5. ϵ Eri (HD 22049)

For this star the stellar parameters found in the literature are again in good agreement. We take the parameters of Santos et al. (2004) ($T_{\rm eff}$ = 5 073 K, log g = 4.42, $\xi_{\rm micro}$=1.05 km s^{-1} and [Fe/H]=–0.13), because these are also the parameters used by Ecuvillon et al. (2004) for their sulphur abundance determination. The projected rotational velocity $V \sin(i)$=3.0 km s^{-1} stems from Nordström et al. (2004).

For this star we measure S/N=300 at 670 nm and a bit smaller than 300 at 870 nm, but S/N=50 at 1045 nm. The results are reported in Table 6. The 3D abundance correction given in column (5) is the one for a star with $T_{\rm eff}$ = 5000 K, log g=4.44 and solar metallicity.

Also for this star the contribution of the iron line to the 1045.5 nm blend of Mult. 3 is high (12 % of the whole line), therefore we exclude this line from the S abundance determination. The error of A(S) according to formula (1) can be found in Table 6, last column.

The LTE sulphur abundance is: A(S)=7.208 ± 0.048, with NLTE correction 7.185 ± 0.067. A(S)=7.148 ± 0.061 if we consider the two lines of Mult. 3, to be compared with 7.241±0.010 from the 675.7 nm and 869.4 nm lines. For this star the agreement of the S abundance derived from the lines of Mult. 3 with that derived from other lines is worse than for other stars. We note also that the lines of Mult. 3 in the observed spectrum appear somewhat distorted and a higher S/N spectrum would be desirable to verify this result.

8. Discussion

The main interest of this investigation is the level of concordance of the abundances derived from the lines of Mult. 3 with the abundances derived from lines of other multiplets. Our results are summarised in Fig. 6, where the value of A(S) for each line is plotted for all stars. There is no evident trend of A(S) with respect to the line used to obtain the abundance, except for the Sun, for which we have noted the strong A(S)-EW correlation. At this stage it is not clear if accounting for NLTE effects in the 3D model may solve this problem. However, the
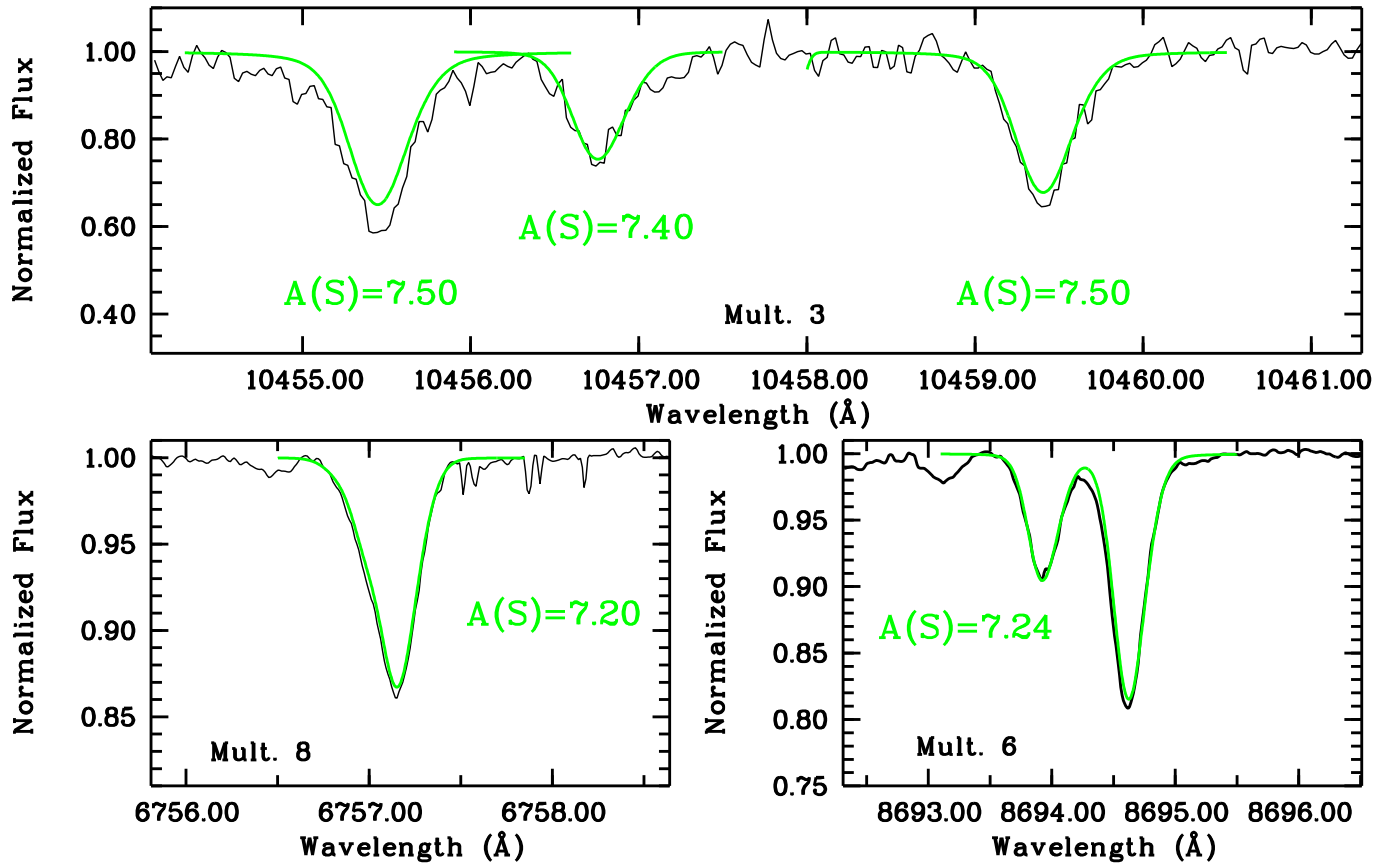
Fig. 5. Procyon: synthetic spectra (green thick line) based on the 3D model are over-imposed on the observed (black solid line) ones.

Table 4. Sulphur abundances in HD 33256. Col. (1) is the wavelength of the line; col. (2) is the Equivalent Width; col. (3) is A(S) from ATLAS+Linfor3D; col. (4) is A(S) from LHD+Linfor3D; col. (5) is A(S) from fitting using an ATLAS+SYNTHE grid; col. (6) is the NLTE correction from Takeda et al. (2005a); col. (7) is the adopted A(S); col. (8) is the statistical error of A(S).

Wave (nm)	EW (pm)	A(S)			Δ FIT	A(S)	σ
		ATLAS	LHD				
(1)	(2)	(3)	(4)	(5)	(6)	(7)	(8)
675.7	2.37	6.822	6.863	6.802		6.863	0.004
869.3	1.63	6.884	6.925	6.895	−0.031	6.894	0.004
869.4	3.92	6.844	6.872	6.895	−0.044	6.828	0.004
1045.5	16.74	7.349	7.300	7.219	−0.239	7.061	0.079
1045.6	7.65	6.977	6.974	7.022	−0.159	6.815	0.116
1045.9	13.35	7.236	7.196	7.119	−0.258	6.938	0.081

good agreement obtained for the other stars is encouraging and suggests that S I Mult. 3 is indeed a valuable abundance indicator. The fact that these abundances are consistent for stars of different spectral types suggests that all the oscillator strength are on the same scale and there is no systematic difference between the different multiplets. We repeat that the error of the log gf for all lines used here is of the order of 50 %, and better

laboratory or theoretical oscillator strengths would be highly desirable.

There is a tendency to underestimate the EWs when the observed spectrum is broadened by an instrumental profile. Tests on strong solar lines, for which we have a very high S/N spectrum show a lower value for the measurements of the EW of more than 3 %, when broadened to a resolution of R~ 80 000.

Table 5. Sulphur abundances in HD 25069. The format is identical to Tab. 4.

Wave (nm)	EW (pm)	A(S) linfor		FIT	Δ	A(S)	σ
		ATLAS	LHD				
(1)	(2)	(3)	(4)	(5)	(6)	(7)	(8)
675.7	1.35	7.277	7.290	7.249		7.290	0.010
869.4	1.60	7.204	7.222	7.204	−0.023	7.199	0.009
1045.6	4.20	7.351	7.372		−0.074	7.298	0.087
1045.9	5.36	7.111	7.132		−0.092	7.040	0.091

Table 6. Sulphur abundances in ϵ Eri (HD 22049). Col. (1) is the wavelength of the line; col. (2) is the Equivalent Width; col. (3) is A(S) from ATLAS+Linfor3D; col. (4) is A(S) from LHD+Linfor3D; col. (5) is A(S) from fitting using an ATLAS+SYNTHE grid; col. (6) is the 3D correction as 3D-LHD for a model of $T_{\mathrm{eff}} = 5000$ K, $\log g = 4.44$ and solar metallicity; col. (7) is the NLTE correction from Takeda et al. (2005a); col. (8) is the adopted A(S); col. (9) is the statistical error of A(S).

Wave (nm)	EW (pm)	A(S)			3D-1D FIT	Δ	A(S)	σ
		ATLAS	LHD					
(1)	(2)	(3)	(4)	(5)	(6)	(7)	(8)	(9)
675.7	0.62	7.162	7.234	7.080	−0.0360		7.234	0.025
869.4	1.02	7.183	7.252	7.047	−0.0304	−0.004	7.248	0.023
1045.5	5.81	7.092	7.143		0.0268	−0.047	7.096	0.035
1045.6	2.52	7.175	7.240		−0.0056	−0.025	7.215	0.082
1045.9	4.36	7.111	7.169	7.047	0.0033	−0.037	7.132	0.057

When dealing with an observed spectrum of lower quality we expect this effect to be even larger. According to our simulations an IR low quality (S/N=20) spectrum can lead to measure an EW of a strong line which is 10 % smaller than the true value, because the wings are lost in the noise.

Our main conclusion is that Mult. 3 can be used successfully to measure the sulphur abundance in the sample of stars we have considered in this work. We believe that this analysis can be extended to metal-poor stars, where the measurement of Mult. 3 lines with the IR spectrograph CRIRES seems particularly promising.

References

Ali, A. W. & Griem, H. R. 1965, Physical Review, 140, 1044

Allende Prieto, C., Asplund, M., López, R. J. G., & Lambert, D. L. 2002, ApJ, 567, 544

Allende Prieto, C., García López, R. J., Lambert, D. L., & Ruiz Cobo, B. 2000, ApJ, 528, 885

Alonso, A., Arribas, S., & Martinez-Roger, C. 1996, A&AS, 117, 227

Anstee, S. D. & O'Mara, B. J. 1995, MNRAS, 276, 859

Asplund, M., Grevesse, N., & Sauval, A. J. 2005, in ASP Conf. Ser. 336: Cosmic Abundances as Records of Stellar Evolution and Nucleosynthesis, ed. T. G. Barnes, III & F. N. Bash, 25

Aufdenberg, J. P., Ludwig, H.-G., & Kervella, P. 2005, ApJ, 633, 424

Bagnulo, S., Jehin, E., Ledoux, C., et al. 2003, The Messenger, 114, 10

Barbuy, B. 1988, A&A, 191, 121

Barklem, P. S., Anstee, S. D., & O'Mara, B. J. 1998a, Publications of the Astronomical Society of Australia, 15, 336

Barklem, P. S. & O'Mara, B. J. 1997, MNRAS, 290, 102

Barklem, P. S., O'Mara, B. J., & Ross, J. E. 1998b, MNRAS, 296, 1057

Barklem, P. S., Piskunov, N., & O'Mara, B. J. 2000, A&A, 363, 1091

Benedict, G. F., McArthur, B. E., Gatewood, G., et al. 2006, AJ, 132, 2206

Bensby, T., Feltzing, S., & Lundström, I. 2003, A&A, 410, 527

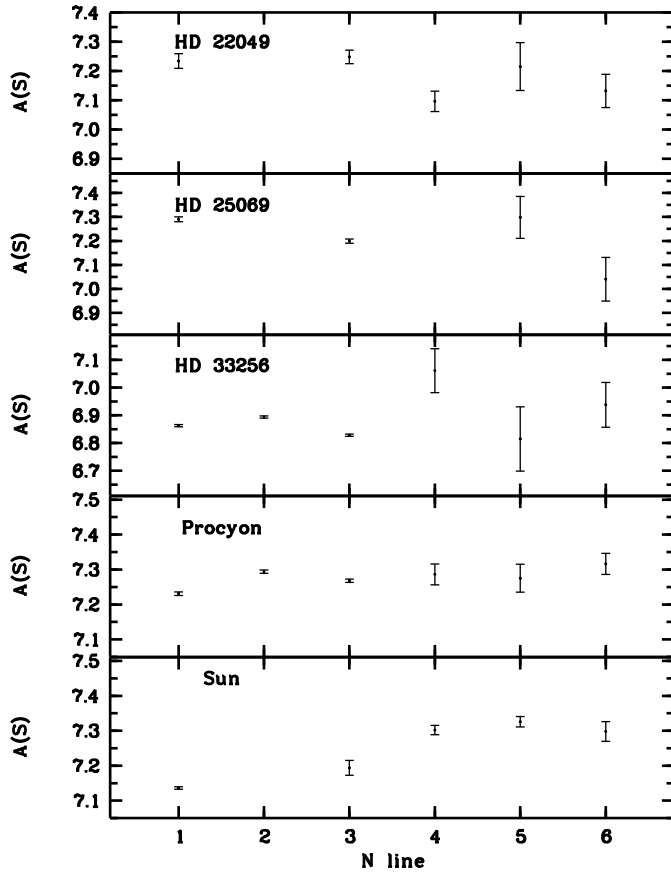Bonifacio, P., Molaro, P., Sivarani, T., et al. 2007, A&A, 462, 851

Fig. 6. For each star, A(S) is plotted as a function of the number of the line: 1 is the 675.7 nm triplet, 2 the 869.3 nm line, 3 the 869.4 nm line, 4 the 1045.5 nm line, 5 the 1045.6 nm line and 6 the 1045.9 nm line. For the Sun the error bar is related to the statistical error coming from the two observed flux spectra. For the other stars it is related to the S/N through Eq. (1).

Bonifacio, P., Sbordone, L., Marconi, G., Pasquini, L., & Hill, V. 2004, A&A, 414, 503

Brown, E. F., Calder, A. C., Plewa, T., et al. 2005, Nuclear Physics A, 758, 451

Brown, R. H., Davis, J., Allen, L. R., & Rome, J. M. 1967, MNRAS, 137, 393

Caffau, E., Bonifacio, P., Faraggiana, R., et al. 2005, A&A, 441, 533

Campbell, B., Walker, G. A. H., & Yang, S. 1988, ApJ, 331, 902

Castelli, F. & Kurucz, R. L. 2003, in IAU Symposium, ed. N. Piskunov, W. W. Weiss, & D. F. Gray, 20P

Cayrel, R. 1988, in IAU Symp. 132: The Impact of Very High S/N Spectroscopy on Stellar Physics, ed. G. Cayrel de Strobel & M. Spite, 345

Cayrel, R., Depagne, E., Spite, M., et al. 2004, A&A, 416, 1117

Centurión, M., Bonifacio, P., Molaro, P., & Vladilo, G. 2000, ApJ, 536, 540

Chen, Y. Q., Nissen, P. E., Benoni, T., & Zhao, G. 2001, A&A, 371, 943

Chieffi, A. & Limongi, M. 2004, ApJ, 608, 405

Clegg, R. E. S., Tomkin, J., & Lambert, D. L. 1981, ApJ, 250, 262

di Benedetto, G. P. 1998, A&A, 339, 858

Drake, J. J. & Smith, G. 1993, ApJ, 412, 797

Ecuvillon, A., Israelian, G., Santos, N. C., et al. 2004, A&A, 426, 619

Edvardsson, B., Andersen, J., Gustafsson, B., et al. 1993, A&A, 275, 101

Freytag, B., Steffen, M., & Dorch, B. 2002, Astronomische Nachrichten, 323, 213

Friel, E. D. & Boesgaard, A. M. 1992, ApJ, 387, 170

Fuhrmann, K. 1998, A&A, 338, 161

Fuhrmann, K., Axer, M., & Gehren, T. 1994, A&A, 285, 585

Garnett, D. R. 1989, ApJ, 345, 282

Gatewood, G. & Han, I. 2006, AJ, 131, 1015

Girard, T. M., Wu, H., Lee, J. T., et al. 2000, AJ, 119, 2428

Gratton, R. G., Carretta, E., & Castelli, F. 1996, A&A, 314, 191

Gratton, R. G., Carretta, E., Desidera, S., et al. 2003, A&A, 406, 131

Gray, D. F. 1981, ApJ, 251, 152

Gray, R. O., Corbally, C. J., Garrison, R. F., McFadden, M. T., & Robinson, P. E. 2003, AJ, 126, 2048

Grevesse, N. & Sauval, A. J. 1998, Space Science Reviews, 85, 161

Hanbury Brown, R., Davis, J., & Allen, L. R. 1974, MNRAS, 167, 121

Holweger, H. 1967, Zeitschrift fur Astrophysik, 65, 365

Holweger, H. & Mueller, E. A. 1974, Sol. Phys., 39, 19

Iwamoto, K., Brachwitz, F., Nomoto, K., et al. 1999, ApJS, 125, 439

Kato, K. & Sadakane, K. 1982, A&A, 113, 135

Kato, K.-I., Watanabe, Y., & Sadakane, K. 1996, PASJ, 48, 601

Kervella, P., Thévenin, F., Morel, P., et al. 2004, A&A, 413, 251

King, J. R. & Boesgaard, A. M. 1995, AJ, 109, 383

Kurucz, R. 1993a, ATLAS9 Stellar Atmosphere Programs and 2 km/s grid. Kurucz CD-ROM No. 13. Cambridge, Mass.: Smithsonian Astrophysical Observatory, 1993., 13

Kurucz, R. 1993b, SYNTHE Spectrum Synthesis Programs and Line Data. Kurucz CD-ROM No. 18. Cambridge, Mass.: Smithsonian Astrophysical Observatory, 1993., 18

Kurucz, R. L. 2005a, Memorie della Società Astronomica Italiana Supplement, 8, 14

Kurucz, R. L. 2005b, Memorie della Società Astronomica Italiana Supplement, 8, 189

Lambert, D. L., Heath, J. E., & Edvardsson, B. 1991, MNRAS, 253, 610

Lambert, D. L. & Luck, R. E. 1978, MNRAS, 183, 79

Limongi, M. & Chieffi, A. 2003a, ApJ, 592, 404

Limongi, M. & Chieffi, A. 2003b, Memorie della Societa Astronomica Italiana Supplement, 3, 58

Luck, R. E. & Heiter, U. 2005, AJ, 129, 1063

Ludwig, H.-G., Jordan, S., & Steffen, M. 1994, A&A, 284, 105

Mihalas, D. 1978, Stellar atmospheres 2nd edition (San Francisco, W. H. Freeman and Co., 1978. 650 p.)

Monaco, L., Bellazzini, M., Bonifacio, P., et al. 2005, A&A, 441, 141

Moore, C. E. 1945, Contributions from the Princeton University Observatory, 20, 1

Mozurkewich, D., Armstrong, J. T., Hindsley, R. B., et al. 2003, AJ, 126, 2502

Mozurkewich, D., Johnston, K. J., Simon, R. S., et al. 1991, AJ, 101, 2207

Neckel, H. & Labs, D. 1984, Sol. Phys., 90, 205

Nissen, P. E. 1981, A&A, 97, 145

Nissen, P. E., Chen, Y. Q., Asplund, M., & Pettini, M. 2004, A&A, 415, 993

Nomoto, K., Thielemann, F.-K., & Wheeler, J. C. 1984, ApJ, 279, L23

Nordgren, T. E., Sudol, J. J., & Mozurkewich, D. 2001, AJ, 122, 2707

Nordlund, Å. 1982, A&A, 107, 1

Nordström, B., Mayor, M., Andersen, J., et al. 2004, A&A, 418, 989

Ozernoy, L. M., Gorkavyi, N. N., Mather, J. C., & Taidakova, T. A. 2000, ApJ, 537, L147

Quillen, A. C. & Thorndike, S. 2002, ApJ, 578, L149

Ramírez, I. & Meléndez, J. 2005, ApJ, 626, 465

Reiners, A. & Schmitt, J. H. M. M. 2003, A&A, 398, 647

Ryan, S. G. 1998, A&A, 331, 1051

Santos, N. C., Israelian, G., & Mayor, M. 2001, A&A, 373, 1019

Santos, N. C., Israelian, G., & Mayor, M. 2004, A&A, 415, 1153

Sbordone, L. 2005, Memorie della Societa Astronomica Italiana Supplement, 8, 61

Sbordone, L., Bonifacio, P., Castelli, F., & Kurucz, R. L. 2004, Memorie della Societa Astronomica Italiana Supplement, 5, 93

Shao, M., Colavita, M. M., Hines, B. E., et al. 1988, ApJ, 327, 905

Steffen, M. 1985, A&AS, 59, 403

Steffen, M. & Holweger, H. 2002, A&A, 387, 258

Takada-Hidai, M., Takeda, Y., Sato, S., et al. 2002, ApJ, 573, 614

Takeda, Y., Hashimoto, O., Taguchi, H., et al. 2005a, PASJ, 57, 751

Takeda, Y., Kato, K.-I., Watanabe, Y., & Sadakane, K. 1996, PASJ, 48, 511

Takeda, Y., Kawanomoto, S., Takada-Hidai, M., & Sadakane, K. 1998, PASJ, 50, 509

Takeda, Y., Ohkubo, M., Sato, B., Kambe, E., & Sadakane, K. 2005b, PASJ, 57, 27

Tomkin, J., Lambert, D. L., & Balachandran, S. 1985, ApJ, 290, 289

Valenti, J. A. & Fischer, D. A. 2005, ApJS, 159, 141

Venn, K. A., Irwin, M., Shetrone, M. D., et al. 2004, AJ, 128, 1177

Vidal, C. R., Cooper, J., & Smith, E. W. 1973, ApJS, 25, 37

Vögler, A., Bruls, J. H. M. J., & Schüssler, M. 2004, A&A, 421, 741

Wedemeyer, S., Freytag, B., Steffen, M., Ludwig, H.-G., & Holweger, H. 2004, A&A, 414, 1121

Wiese, W. L., Smith, M. W., & Miles, B. M. 1969, Atomic transition probabilities. Vol. 2: Sodium through Calcium. A critical data compilation (NSRDS-NBS, Washington, D.C.: US Department of Commerce, National Bureau of Standards,)

Woosley, S. E. & Weaver, T. A. 1995, ApJS, 101, 181

Zhao, G. & Magain, P. 1991, A&A, 244, 425

Appendix A: Remarks on individual stars

1. Sun:
   The 675.7 nm sulphur triplet is not blended and it is well reproduced in comparison with synthetic spectra, when using the atomic data reported in Table 1. We do not consider the sulphur triplet at 674.3 nm whose shape in the solar observed spectra is not well reproduced, perhaps due to blending by a CN line. The 674.8 nm sulphur triplet is also discarded because of a blend with vanadium, calcium, iron and titanium whose atomic data are not well known.
   The two sulphur lines of Mult. 6 in the range 870 nm are both well reproduced by synthetic spectra. The lines are situated very close to each other, so in the 1D analysis we fitted both simultaneously. In the 3D analysis we concentrated on the 869.4 nm line. The 869.3 nm line is blended with molecules (CN and C_2), and it is weaker than the 879.4 nm line. We computed the EW of the contribution of molecules in the range of this line to derive the sulphur abundance from this line.
   We do not consider in this work the Mult. 1 (920 nm) sulphur lines, because they are affected by telluric lines. The 922.8 nm line is the cleanest among the three lines, but it lies in the wing of the Paschen ζ H-line, so the abundance analysis is not free from possible systematic errors.

2. Procyon:
   Allende Prieto et al. (2002) and later Aufdenberg et al. (2005) investigated Procyon's limb darkening with 3D models. Both groups found that 3D models predict a smaller degree of limb darkening than 1D models. Aufdenberg et al. showed that an approximate overshooting introduced in 1D Phoenix or ATLAS models can largely eliminate these differences. The case of Procyon is fortunate because it is a well studied visual binary system. The mass of the primary is well determined (see Gatewood & Han 2006 and Girard et al. 2000 for the most recent astrometric studies of this star).
   The angular diameter has been measured directly by Brown et al. (1967); Hanbury Brown et al. (1974) and, more recently, by Shao et al. (1988); Mozurkewich et al. (1991);

di Benedetto (1998); Nordgren et al. (2001); Mozurkewich et al. (2003); Kervella et al. (2004).

The distance from Hipparcos and orbital motion studies are reported in Gatewood & Han (2006).

The surface gravity of this star is well known from the orbital data and diameter measurements: $\log g = 4.0$ with an error less than 0.1, in agreement with Allende Prieto et al. (2002), who obtained $\log g = 3.96 \pm 0.02$.

The effective temperature depends on the method used to derive it. Critical reviews of values obtained by various authors with different methods are summarised in Steffen (1985) and in Kato et al. (1996). The T_{eff} values range from 6 400 K (the lowest value derived from the continuum and IR fluxes) to more than 6 800 K (from the ionisation balance of Fe). By excluding the high values derived from line spectrum analysis, the highest T_{eff} value depends on the value of the mixing-length adopted in the models; a lower mixing-length corresponds to a lower convective flux so to a higher temperature gradient at the bottom of the the atmosphere (Kato & Sadakane 1982). A synthetic spectrum at an effective temperature of 6 500 K with $\alpha_{\mathrm{MLT}} = 0.5$ agrees with Balmer line profiles (Fuhrmann et al. 1994).

We give more weight to the value derived from the flux distribution, adopt 6 500 K and ascribe the higher values required to fit the ionisation balance to the inaccuracy of the structure of the atmosphere adopted in 1D models. These models require a higher T_{eff} to describe the outer atmospheric layers where the lines are formed.

A further proof of the inadequacy of the structure of the 1D models is given by the extensive discussion on the derivation of the atmospheric parameters by Luck & Heiter (2005) based on the choice of the model that better fits the spectroscopic data; they obtain $T_{\mathrm{eff}} = 6850$ K, $\log g = 4.55$, $\xi_{\mathrm{micro}} = 2.4$ km s^{-1}.

A selection of stellar parameters from the literature is given in Table A.1.

3. HD 33256:
   HD 33256 is slightly cooler than Procyon (F5 IV-V) in spite of the earlier spectral type given in Simbad and the Bright Star Catalog (BSC), F2V. It is slightly metal deficient and so has weaker lines than a solar abundance star. This is at the origin of its earlier than Procyon's spectral type. In fact the new accurate classification by Gray et al. (2003) is F5.5V (kF4, mF2).

   It is not far from the Galactic plane, in fact its Galactic coordinates are: 208.83, –24.83. It is a thin disk star according to Bensby et al. (2003). The S abundance has been measured by Takada-Hidai et al. (2002). These authors adopted [Fe/H] from Edvardsson et al. (1993), while they derived temperature and gravity (see Table A.2). The LTE derived S abundance, based on the 8 693 nm and 8 694 nm lines, is 7.29. A selection of stellar parameters is listed in Table A.2.

4. HD 25069:

No detailed abundance analysis has been done for this star, but many measures of its radial velocity exist up to 2005. Valenti & Fischer (2005) made an extensive study of the spectroscopic properties of cool stars. From one Keck spectrum they derived (with Kurucz models): $T_{\mathrm{eff}} = 4\,994$ K, $\log g = 3.53$, [M/H] = 0.10, $V \sin(i) = 3.3$ km s^{-1}, RV = 39.2 km s^{-1}. Abundances of Na, Si, Ti, Fe, Ni are also given. The star seems to be cooler than spectral type G9, as found in Simbad data base. We keep the stellar parameters from Valenti & Fischer (2005).

It is remarkable that, although for such a cool star the Hα profile is very little sensitive to effective temperature, from the fitting of the wings of Hα we obtain: $T_{\mathrm{eff}} = 4\,726$ K, which is in very good agreement with the temperature derived from the B-V colour: B-V=1.00 implies $T_{\mathrm{eff}} = 4\,700$ K.

5. ϵ Eri:
   ϵ Eri (HD 22049) is a much studied star (795 papers since 1983). It is a variable star of BY Dra type (BY Dra stars are flare stars with cool spots, which cause photometric variations during the rotation of the star). It has two suspected planets: ϵ Eri b (Campbell et al. 1988), ϵ Eri c (Quillen & Thorndike 2002). Benedict et al. (2006) determined the mass of ϵ Eri b from HST and ground-based astrometric and RV data, modelled its orbit, confirmed the existence of this companion and discuss the existence of the possible tertiary invoked by Quillen & Thorndike (2002) and Ozernoy et al. (2000). The star has a high level of magnetic activity inferred from chromospheric activity consistent with a relatively young age, less than 1 Gyr. Observational and theoretical searches for the signature of planetary/brown dwarf objects in the structure of the dust disk around this star are underway by Benedict et al. (2006). A selection of stellar parameters is listed in Table A.3.

List of Objects

Table A.1. Procyon: stellar parameters with reference.

T_{eff} K	$\log g$	[Fe/H] km s^{-1}	ξ_{micro} km s^{-1}	$V \sin(i)$	Reference
				2.8	Gray (1981)
6500 ± 80	4.0 ± 0.1		2.1 ± 0.3	< 4.5	Steffen (1985)
6605	4.13	–0.06	2.23		Gratton et al. (1996)
6500	4.00		1.4	3.3	Takeda et al. (1996)
6470	4.01 ± 0.10	-0.01 ± 0.07	1.91 ± 0.20	2.6 ± 1.0	Fuhrmann (1998)
6640	4.13		1.8	6.6	Takeda et al. (1998)
6530 ± 50	3.96 ± 0.02		2.2	3.16 ± 0.5	Allende Prieto et al. (2002)
6543 ± 84	3.975 ± 0.013				Aufdenberg et al. (2005)

Table A.2. Stellar parameters of HD 33256

T_{eff} K	$\log g$	[Fe/H]	ξ_{micro} km s^{-1}	$V \sin(i)$ km s^{-1}	Ref
6 550	4.09	–0.34	1.4		Nissen 1981
6 270	4.0				Clegg et al. 1981
6 270	4.0	–0.26	1.0		Tomkin et al. 1985
6 440	4.05	–0.30			Lambert et al. 1991
6 300	3.60	–0.45	1.40		Zhao & Magain 1991
6 400	3.95	–0.336		0	Friel & Boesgaard 1992
6 442	4.05	–0.30			Edvardsson et al. 1993
6 386	4.10	–0.30	2.10		King & Boesgaard 1995
6 385	4.10	–0.30			Chen et al. 2001
6 440	3.99	–0.30	2.3		Takada-Hidai et al. 2002
6 411	3.87	–0.30	1.5		Gray et al. 2003
6 427	4.04	–0.30	1.90		Bensby et al. 2003
				9.7	Reiners & Schmitt 2003

Table A.3. ϵ Eri (HD 22049): stellar parameters with reference.

T_{eff} K	$\log g$	[Fe/H]	ξ_{micro} km s^{-1}	$V \sin(i)$ km s^{-1}	Reference
5 180	4.75	–0.09	1.25		Drake & Smith (1993)
5 076	4.50	0.05			Alonso et al. (1996)
	4.84			2.1	Allende Prieto et al. (2000)
5 135	4.70	–0.07	1.14		Santos et al. (2001)
5 117				3	Nordström et al. (2004)
5 073	4.43	–0.13	1.05		Santos et al. (2004)
4 992					Ramírez & Meléndez (2005)
5 177	4.72	0.06	0.62		Takeda et al. (2005b)
5 200	4.50	–0.04	0.70		Luck & Heiter (2005)